EUROPEAN FUSION DEVELOPMENT AGREEMENT

EFDA–JET–PR(04)56

P. Monier-Garbet, Ph. Andrew, P. Belo, G. Bonheure, Y. Corre, K. Crombe, P. Dumortier, T. Eich, R. Felton, J. Harling' J. Hogan, A. Huber, S. Jachmich, E. Joffrin, H.R. Koslowski, A. Kreter, G. Maddison, G.F. Matthews, A. Messiaen, M.F. Nave, J. Ongena, V. Parai, M.E. Puiatti, J. Rapp, R. Sartori, J. Stober, M.Z. Tokar, B. Unterberg, M. Valisa, I.Voitsekhovitch, M. von Hellermann and JET-EFDA contributors

# Impurity-Seeded ELMy H-modes in JET, with High Density and Sustainable Heat Load.

# Impurity-Seeded ELMy H-modes in JET, with High Density and Sustainable Heat Load.

P. Monier-Garbet[1], Ph. Andrew[2], P. Belo[3], G. Bonheure[4], Y. Corre[5], K. Crombe[6], P. Dumortier[4], T. Eich[7], R. Felton[2], J. Harling[2], J. Hogan[8], A. Huber[9], S. Jachmich[4], E. Joffrin[1], H.R. Koslowski[9], A. Kreter[9], G. Maddison[2], G.F. Matthews[2], A. Messiaen[4], M.F. Nave[3], J. Ongena[4,10], V. Parai[12], M.E. Puiatti[11], J. Rapp[9,10], R. Sartori[12], J. Stober[7], M.Z. Tokar[9], B. Unterberg[9], M. Valisa[11], I. Voitsekhovitch[2], M. von Hellermann[13], and JET-EFDA contributors*

[1]*Association EURATOM-CEA sur la Fusion Contrôlée, DSM/DRFC, Cadarache, St Paul-lez-Durance, France.*
[2]*UKAEA/Fusion Association, Culham Science Center, Abingdon, OXON, UK.*
[3]*Associaçao Euratom-IST, Centro de Fusao Nuclear, 1049-001 Lisbon, Portugal.*
[4]*LPP- ERM/KMS, Euratom-Belgian State Association, TEC, Brussels, Belgium.*
[5]*Association EURATOM-VR, Royal Institute of Technology, Physic Department, Stockholm, Sweden.*
[6]*Department of Applied Physics, University of Gent, 9000 Gent, Belgium.*
[7]*Max-Planck Institut für Plasmaphysik, Boltzmannstrasse, Garching, Germany.*
[8]*Oak Ridge National Laboratory, USA.*
[9]*Institut für Plasmaphysik, Forschungszentrum Jülich, EURATOM Association, TEC, Jülich, Germany.*
[10]*EFDA, CSU Culham, Abingdon, OXON, UK.*
[11]*Consorzio RFX – Associazione Euratom-Enea sulla Fusione, I-35127 Padova, Italy.*
[12]*EFDA, CSU Garching, Garching, Germany.*
[13]*FOM-Rijnhuizen, Ass. Euratom-FOM, PO Box 1207, 3430 BE Nieuwegein, NL**.*
**See appendix of J. Pamela et al., "Overview of JET results", in Proc of 19th IAEA Fusion EnergyConference, Lyon, 2002 (IAEA, Vienna, 2003)** Partner in the Trilateral Euregio Cluster (TEC)*

Preprint of Paper to be submitted for publication in
Nuclear Fusion

**ABSTRACT.**

Experiments performed at JET during the past two years show that, in high triangularity H-mode plasmas with $I_p$=2.5MA, $n_e/n_{Gr} \approx 1.0$ , it is possible to radiate separately up to ≈ 40% of the total injected power on closed flux surfaces in the pedestal region (argon seeding) and up to ≈ 50% of the injected power in the divertor region (nitrogen seeding), while maintaining the confinement improvement factor at the value required for ITER, H98(y,2) ≈ 1.0. The total radiated power fraction achieved in both cases (65 – 70%) is close to that required for ITER. However, Type I ELMs observed with impurity seeding have the same characteristics as that observed in reference pulses without seeding: decreasing plasma energy loss per ELM with increasing pedestal collisionality. One has to reach the Type III ELM regime to decrease the transient heat load to the divertor to acceptable values for ITER, although at the expense of confinement. The feasibility of an integrated scenario with Type-III ELMs, and $q_{95}$=2.6 to compensate for the low H factor, has been demonstrated on JET. This scenario would meet ITER requirements at 17MA provided that the IPB98 scaling for energy content is accurate enough, and provided that a lower dilution is obtained when operating at higher absolute electron density.

## 1. INTRODUCTION.

In ITER, both the steady-state and the transient heat flux to the divertor will have to be limited to values tolerable for the wall materials ($\Phi$steady-state <10MW/m$^2$ and $\Phi$transient<50MJ/m$^2$/s$^{1/2}$ [1]). This paper reports on the experimental work performed at JET during the past two years to assess the feasibility of an integrated H-mode scenario using impurity seeding to reduce the heat flux to the divertor. A steady-state heat flux less than 10MW/m$^2$ in ITER is calculated to correspond to $P_{rad,tot}/P_{tot} \approx 0.75$, and in the present ITER scenario with C divertor and Be first wall, this is planned to be achieved using argon injection [2, 3], which for ITER pedestal parameters would correspond to high radiation in the divertor region, $0.50 / P_{rad,div} P_{tot} \approx 0.50$, and type I ELMs for good confinement. The 25% remaining radiation fraction is expected to come from bremstrahlung losses in the bulk plasma with $Z_{eff}$=1.7. The work reported here brings new insight into the following issues: 1) is it possible, in high triangularity, high density H-mode plasmas, to achieve $P_{rad,tot}/P_{tot} \approx$ 0.75 together with good confinement? what are the respective contributions of bulk and divertor radiations in this case? what impurity species should be used to obtain this distribution? 2) what is the corresponding ELM regime? can impurity be used to control/mitigate ELMs? Issues 1) and 2) are addressed in sections 2 and 3 respectively.

## 2. STEADY-STATE HEAT FLUX TO THE DIVERTOR AND GLOBAL CONFINEMENT PROPERTIES.

### *A) EXPERIMENTAL CONDITIONS.*

Argon and nitrogen impurities have been injected in high density high triangularity H-mode plasmas in JET. In the argon seeding scenario, the radiated power and the confinement improvement factor

are controlled simultaneously by the argon and deuterium injection rates through a feedback loop [4]. The plasma current and toroidal field are $I_p$=2.5MA, $B_t$=2.7T corresponding to q=3.6. The total injected power is = 17MW ($P_{NBI}$=14MW + $P_{ICRH}$=3MW). In the nitrogen seeding scenario, the radiated power is feedback controlled by the nitrogen injection rate and a pre-set constant deuterium injection is used. The toroidal field is reduced to 2.0T for q=2.6 [5]. The total injected power is 13MW. This paper compares the results of the argon and nitrogen experiments with the aim of determining the characteristics required for the seed impurity in ITER. Only high triangularity ($\delta$=0.44) plasmas with the MkIISRP divertor configuration, without the septum, are analysed. The best performance obtained so far with impurity seeding is compared to the corresponding JET 'reference' data base with no seeding [6].

***B) RADIATED POWER AND THERMAL CONFINEMENT.***

Figure 1 shows the thermal confinement improvement factor calculated from the IPB98(y,2) scaling law versus the electron density normalized to the Greenwald density (a), the total radiated power (b) and the power radiated in the divertor region (c) both normalized to the total injected power. The radiated power is measured by bolometry. The radiated power in the divertor region ($P_{rad,div}$) shown in Fig.1(c) corresponds to the poloidally asymmetric part of the radiation in the vicinity of the X-point. It is the difference between the total radiated power ($P_{rad,tot}$ ) and the contribution, which is poloidally symmetrical ($P_{rad,bulk}$/ $P_{tot}$ ), and calculated from the bolometer lines of sight viewing the plasma upper half only. Analysis of the detailed tomographic reconstruction of bolometry data indicates that the determination of $P_{rad,div}$ and $P_{rad,bulk}$ as reported above is accurate within ± 10%. Further analysis of the radiation patterns observed with argon or nitrogen seeding is reported in section c) below. The reference data base obtained in high density high triangularity H-modes with no seeding shows that in JET, with carbon divertor and first walls, $P_{rad,div}/P_{tot} \approx 0.30$ and $P_{rad,bulk}/ P_{tot}$ 0.25 (total radiated power fraction $P_{rad,tot}/P_{tot} \approx 0.55$) are currently achieved with H98(y,2) =1.0-1.05. With either argon or nitrogen seeding, a total radiated power fraction $P_{rad,tot}/ P_{tot}$ up to 0.65 – 0.70 (Pulse No: 61371 and Pulse No: 58729) is achieved with a confinement loss limited to ≈ 5% (H98(y,2)~1.0) compared to the best reference H-modes. Consistent with bolometry data, infra-red measurements of the inner target plate surface temperature also indicate a lower heat flux to the inner plate in the impurity seeded scenario, compared to the non-seeded case. Increasing the radiated power fraction, beyond 0.65-0.70 leads to further degradation of the confinement (#60716 and Pulse No: 59029 for argon and nitrogen respectively). Figure 2 analyses the separate effects of deuterium and impurity injection rates on confinement, in argon seeded plasmas. It shows that i) the global confinement decreases with increasing argon injection rate, ii) it decreases more rapidly in the case of a high deuterium injection ($\Phi_{D2} = 7 \times 10^{22}$e/s compared to $\Phi_{D2} = 4 \times 10^{22}$e/s), which is consistent with these different rates producing very similar electron densities in the plasma, iii) even in the case of a low argon injection, corresponding to discharges in which H98(y,2) is still close to 1.0, the 5% confinement loss in these pulses is correlated to the impurity injection, and may not be attributed to a strong deuterium injection.

The degradation of the global confinement observed at high radiated power fractions is correlated with a decrease of the pedestal electron temperature, as illustrated by the pedestal ($T_e$, $n_e$) diagram (Fig.3). A total radiated power fraction 0.75 3 -0.80, either with argon or nitrogen radiation brings the pedestal temperature well below the level usually observed in good H-mode confinement pulses. The transition towards lower confinement occurs at a higher value of $P_{rad,bulk}/P_{tot}$ (≈ 40%) with argon than with nitrogen (≈ % 02) since, due to its atomic physics characteristics, argon radiates mainly in the region where $T_e \leq 900$eV, which corresponds to the pedestal temperature for Type I ELMs and good confinement. On the contrary, nitrogen radiates at a lower electron temperature, well within the domain for Type III ELMs. In the high confinement regime with Type I ELMs, the electron temperature profiles, inside the pedestal region, are very similar in cases without and with impurity seeding (Fig.4), which is consistent with the observation that the ratio of pedestal to core energy content is unchanged (Fig.5). This indicates that these impurity seeded pulses do not break the link between the global confinement and the pedestal properties, which is usually observed in JET H-modes. The ELM regimes observed for $P_{rad,tot}/P_{tot} \leq 0.70$ (H98(y,2) ≈0.1 ) and $P_{rad,tot}/P_{tot} \leq 0.75$, (low confinement) will be discussed in section 3. With nitrogen seeding, at the highest achieved radiated power fractions, partially detached divertor conditions are observed. The heat flux density is reduced to about 2-5MW/$m^2$ and electron temperatures in the divertor of less than 10eV are achieved [5]. The reduced normalized confinement observed in these conditions is proposed to be compensated in ITER by operating at high plasma current, $I_p$=17MA. Indeed, the ITER operational domain for Q=10 does allow operation at confinement enhancement factors of H98(y,2) ≈ 0.78 provided the plasma current is increased accordingly. Pulse 59029 shown in Fig.1 demonstrates on JET the feasibility of such an integrated scenario: 2.5MA/2.0T, $q_{95}$=2.6, H98(y,2)=0.73, $P_{rad,tot}/P_{tot}$ = 0.80, $n_e/n_{Gr}$=1.0, $Z_{eff}$=2.1, $\beta_N$=1.7, $\delta$=0.44) [5].

### *C) COMPARISON OF ARGON AND NITROGEN RADIATION PATTERNS.*

Figure 6 shows a few time traces for two H-mode pulses with very similar global characteristics, in particular H98(y,2) ≈ 0.1, Type I ELMs, $P_{rad,tot}/P_{tot}$ = 0.65 - 0.70, except that the seed impurity is different in the two pulses. In the case of argon seeding, most of the radiation is emitted on closed flux surfaces inside the separatrix ($P_{rad,tot}/P_{tot} \approx 0.40$), and ≈ 25% of the total power is radiated in the divertor region. In contrast, with nitrogen seeding, most of the radiation is located in the divertor region, $P_{rad,div}/P_{tot} \approx 0.50$. The two radiation patterns obtained from tomographic reconstruction of bolometry data are shown in Fig.7. The radial profiles of the radiated power density, also from tomographic reconstruction of the bolometry data, are shown in Fig.8, together with the corresponding electron temperature profiles. In the case of argon seeding, the radiative shell extends in the edge region for $\rho > 0.5$ and $T_e <$ 2.0keV, in good qualitative agreement with the radiation of ArXVI ions at coronal equilibrium. The average effective charge measured by visible bremstrahlung is very similar in the two discharges, $Z_{eff} \approx 2.1$ either with argon or nitrogen seeding. Spectroscopic measurements show that, at these high radiative power fractions, the carbon influx from the divertor

is reduced significantly with nitrogen seeding [7], as might be expected from [8]. The intrinsic impurities, mainly C and Be, are replaced by the seed impurity. A detailed modelling of the power radiated by each impurity species is in progress.

## 3. TRANSIENT HEAT FLUX TO THE DIVERTOR DURING ELMS

### *A) SCALING OF TYPE I ELMS PLASMA ENERGY LOSS IN IMPURITY SEEDED PLASMAS.*

Type I and Type III ELM regimes are observed for $0.70\ P_{rad,tot}/P_{tot} \leq 0.70$ (H98(y,2) ≈ 0.1) and $P_{rad,tot}/P_{tot} \leq 0.75$ (low confinement) respectively. This is true for argon and for nitrogen impurities. The precise value of $P_{rad,tot}/P_{tot}$ at the Type I/ III transition is difficult to determine from the available experimental data. In particular, it is not possible to determine from the limited data base analysed here, whether there is a difference between argon and nitrogen, although a higher value of $P_{rad,tot}/P_{tot}$ at the Type I/III transition would be expected with nitrogen since it corresponds a lower power loss channel in the pedestal region. Analysis made so far shows that the Type I ELMs observed with impurity seeding have the same characteristics as that observed in the reference high triangularity pulses without seeding (Fig.9). In particular, the plasma energy loss per ELM, $\Delta W_{ped}/W_{dia}$, decreases with increasing pedestal collisionality [5, 9], following the empirical scaling found in [3]. These results show that impurity seeding may be used as an additional tool to control the pedestal collisionality, at the expense of a reduced pedestal temperature. The frequency of the Type I ELMs observed with argon seeding decreases with increasing $P_{rad,bulk}$ , i.e. decreasing conductive power across the separatrix. Predictive modelling with the JETTO code shows that the decreased frequency is due to a decreased power across the separatrix rather than a higher threshold for ballooning instability which might have been associated to increased $Z_{eff}$.

### *B) RADIATION BUFFERING OF TYPE I ELMS.*

Experimental work has also been done on JET [10] to determine the conditions in which part of the released ELM energy can be dissipated by radiation in the Scrape Off Layer and divertor regions before reaching the target plates ('buffering' effect). For diagnostic purposes, these experiments have been done in a low triangularity shape plasma ($\delta \approx 0.26$). N or Ar impurities are injected in Type-I ELMy H-modes up to a radiative power fraction of ~55%. The heat load to the target plates, during and in between ELMs, is measured using a fast infra-red camera [11]. The presence of a codeposited layer on the inner target is taken into account to calculate the deposited energy and heat fluxes from the surface temperature measurement [12]. Figure 10 shows the plasma energy loss, from fast diamagnetic measurements ($\Delta W_{dia}$), and the corresponding energy increase on the outer target plate for a typical event. The Type I ELMs analysed here correspond to $\Delta W_{dia}$ up to 500kJ. Only a very small fraction of the ELM energy is found to be radiated before reaching the target plates: the energy increase on the target plate normalized to the plasma energy loss during an ELM ($\Delta W_{target}/\Delta W_{dia}$) is marginally reduced (by 18 - 24% on the outer and inner targets respectively)

compared to non seeded reference pulses (Fig.11). However, experimental evidence of buffering of small type III ELMs is found in the nitrogen seeded pulses [5] at radiative power fractions above 80%. In these experiments, complete detachment in between ELMs is achieved by fuelling the plasma with deuterium and nitrogen. Both the transient power load to the divertor and the plasma energy loss due to ELMs are decreased (Type III ELM regime, $\Delta W_{dia}$ ~25kJ, $\Delta W/W$~0.7%).

***C) MODELLING.***

The above experimental results are supported by time-dependent SOLPS5.0 modelling [13]. The core plasma is described using the MIST and SANCO impurity transportcodes. These include an ELM model in which impurities are assumed to be instantaneously expelled into the SOL from the ELM-affected region and then recycled. The edge region (both the SOL and pedestal) is modelled using the time-dependent SOLPS5.0 code. Deuterium plus two impurity species, C and N are included. ELMs are described by increased heat and particle perpendicular diffusivities compared to steady-state values. Enhancement factors of 50 and 100 have been used : these values correspond to the same ELM energy loss in the experiment (there is a fixed amount of $\Delta W_{dia}$ which can be removed, 350-400 kJ in the case considered), but the higher enhancement case removes the energy faster, and the time to remove it is smaller. Figure 12 shows the calculated electron energy hitting the divertor target normalized to that crossing the separatrix, versus the time needed to remove the energy from the pedestal ($\tau_{ELM}$, determined by the enhancement factor). The background plasma conditions are those of the pulses described above, Pulse No: 58135 reference case without impurity seeding, and Pulse No: 58139 with N seeding. Although the calculated fraction of the ELM energy reaching the target is smaller than that actually observed, the reduction of ≈ 15% of $\Delta W_{target}/\Delta W_{SOL}$ with N seeding which is calculated for $\tau_{ELM} \approx 150\mu s$ is consistent with the experimental findings, and with previous code results [3, 5], predicting that a significant effect could only be obtained for very small ELMs ($\Delta W_{dia} < 0.6$MJ in ITER). Note that a stronger reduction is predicted for a longer ELM. SOLPS5.0 has also been used to perform a study of the sensitivity of the bolometric measurements to the expected increase of N radiation associated to ELM buffering. Figure 13 shows that this increase is likely to be too small and localised in time to be detected by the bolometers with a 20ms integration time.

## 4. DISCUSSION AND CONCLUSION

***A) STEADY-STATE HEAT FLUX TO THE DIVERTOR.***

Analysis of JET high triangularity H-mode experiments with $I_p$=2.5MA, $n_e/n_{Gw} \approx 1.0$ , shows that, provided that the appropriate impurity species is chosen, Ar and N respectively for JET plasma conditions, it is possible to radiate separately up to ≈ 40% of the total injected power on closed flux surfaces in the pedestal region and up to 50% of the injected power in the divertor region, while maintaining the confinement factor close to that required for ITER. In both cases, $P_{rad,tot}/P_{tot} \approx$ 0.65 - 0.70. Increasing the radiation level above this value leads to a degradation of the pedestal

parameters, Type III ELM regime, and reduced confinement. Indeed, the increase in radiation is associated with a reduced pedestal energy, and the fraction of energy in the pedestal ($W_{ped}/W_{tot}$) is the same, for a given confinement level, with and without impurity seeding. Predicting the corresponding maximum values of $P_{rad,bulk}/P_{tot}$ and $P_{rad,div}/P_{tot}$ achievable in ITER together with good confinement remains however uncertain, as the relation between divertor and pedestal electron density and temperature is different in JET and ITER, and the non-dimensional parameters of the experiments analyzed here are not that of ITER plasmas. In this respect, experiments in JET at higher plasma current ($\geq$ 3.0MA), and consequently higher absolute density would bring valuable additional information on the scaling with current and input power of the limits in $P_{rad,bulk}/P_{tot}$ and $P_{rad,div}/P_{tot}$, which are achievable with good confinement. Another option to be explored in order to increase further the radiated power and maintain the confinement could be to increase the actual volume used for radiation by combining two impurity species, one radiating at the temperature of the top of the pedestal to produce $P_{rad,bulk}/P_{tot} \leq 0.40$, and the other one radiating at lower temperature, in the divertor region to produce $P_{rad,div}/P_{tot} \leq 0.50$. However, for the scenario involving high radiation on closed flux surfaces inside the separatrix, two further issues have still to be assessed carefully: the proximity to the H to L power threshold ($P_{L-H} \propto n_e$), and the net decrease of heat flux to the divertor that the scenario would bring (higher injected power, to compensate for the power radiated inside the separatrix).

***B) TRANSIENT HEAT FLUX TO THE DIVERTOR DURING TYPE I ELMS.***

As shown in Fig. 3, the operational domain with impurity seeding and good confinement corresponds to the Type I ELM domain. The normalized plasma energy loss ($\Delta W_{dia}/W_{ped}$) during Type I ELMs follows the same scaling with the pedestal collisionality, without and with impurity seeding. As for a possible radiative dissipation of the Type I ELM energy in the SOL and divertor regions before reaching the target plates, experiments and modelling on JET show that only a very small fraction of Type I ELM energy might be radiated. As a consequence, we do not expect large ELM buffering in ITER except for very small ELMs. In conclusion, there is no experimental evidence so far of any strong reduction of the transient heat flux to the divertor during Type I ELMs with impurity seeding. One has to reach the Type III ELM regime to decrease the transient heat load to the divertor to acceptable values for ITER.

Finally, on the basis of the experimental results discussed above, two options using impurity seeding may be further considered for an integrated scenario for ITER: 1) use impurity injection to obtain $P_{rad,tot}/P_{tot} \approx 0.75$ with H98(y,2) $\approx$ 1.0, but one needs a separate technique to mitigate the Type I ELMs, 2) use a Type III ELM regime with impurity seeding, to obtain sustainable steady-state and transient heat loads to the divertor, although at the expense of confinement. The feasibility of such an integrated scenario has been demonstrated on JET: 2.5MA/2.0T, $q_{95}$=2.6, H98(y,2)=0.73, $P_{rad,tot}/P_{tot} \approx 0.80$ , $n_e/n_{Gr}$=1.0, $Z_{eff}$=2.1, $\beta_N$=1.7, $\delta$=0.44) [5]. It would meet ITER requirements at 17MA provided that the ITER98 scaling for energy content is accurate enough, and provided that a lower dilution is obtained when operating at higher absolute electron density.

**REFERENCES**


[1]. G. Federici, et al., J. Nucl. Mat. 313-316 (2003) 11-22.

[2]. A.S. Kukushkin, H D Pacher, Plasma Phys Cont Fusion **44** (2002) 931-943

[3]. A. Loarte, et al., Proc. 18th IAEA Fusion Energy Conf., Sorrento (2000).

[4]. P. Dumortier, et al., Procceedings of 31st EPS Conf., London, 28 June-2 July (2004) P5.170.

[5]. J. Rapp, et al., Nucl. Fusion 44 (2004) 312-319.

[6]. R. Sartori, et al., PPCF **44** (2002) 1801-1813.

[7]. J. Rapp, et al., J. Nucl. Mat.(2004), Proceedings PSI Conf.

[8]. F. L. Tabares, et al., 31st EPS Conf., London, 28 June-2 July (2004).

[9]. G. Maddison, et al., PPCF **45** (2003) 1657.

[10]. P. Monier-Garbet, et al., 30th EPS Conf. on Controlled Fusion and Plasma Physics, St Petersburg, Russia, 7-11 July 2003.

[11]. T.H. Eich, et al., J. Nucl. Mat. **313-316** (2003) 919-924.

[12]. Y. Corre, et al., 30th EPS Conf. on Controlled Fusion and Plasma Physics, St Petersburg, Russia., 7-11 July 2003.

[13]. D. COSTER, et al, J. Nucl Mat. **313-316** (2003) 868.

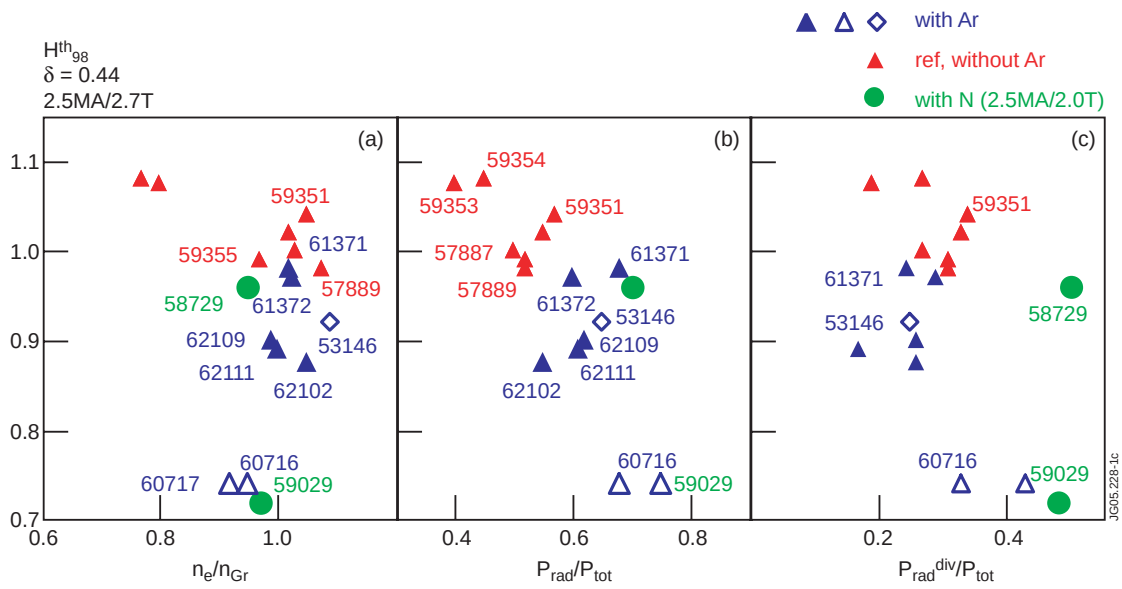


*Figure 1: Thermal confinement factor versus a) fraction of Greenwald density, b) total radiated power fraction, and c) fraction of input power radiated in the divertor region. The open symbols correspond to pulses in which steady-state is not achieved, and the diamond symbol corresponds to ahigh triangularity pules, but with a slightly different magnetic configuration*

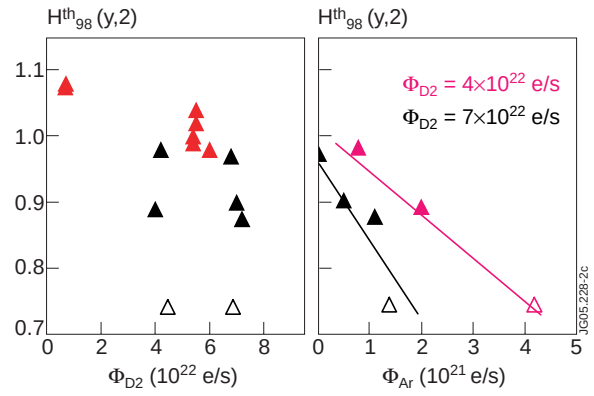


*Figure 2: Thermal confinement factor versus deuterium injection rate (left), and versus argon injection rate (right) for two values of the deuterium injection.*

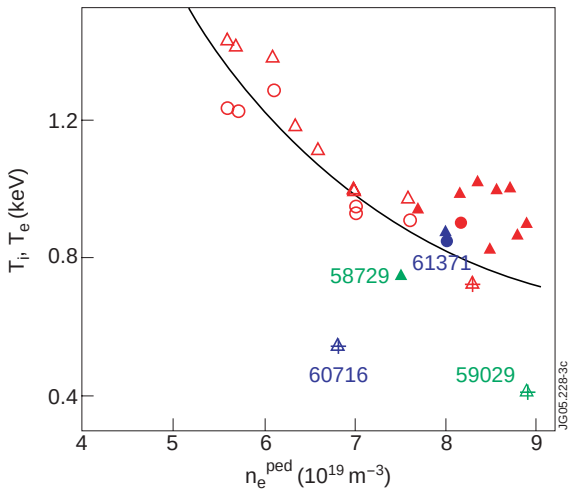


*Figure 3: Pedestal ($n_e$, $T_e$) for Type I and TypeIII ELMs for high triangularity pulses, 2.5MA/2.7T. △ = $T_i$, ○ = $T_e$, red = reference pulses (no impurity seeding), full symbols correspond to mixed TypeI/II ELMs, blue(green)=Ar(N) seeding.*

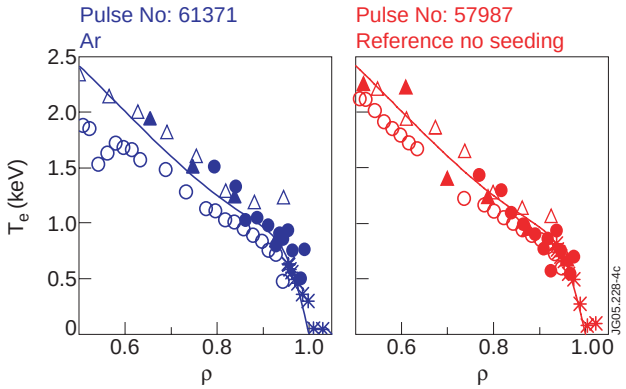


*Figure 5: Electron temperature profiles of two pulses shown in Fig.1, with H98(y,2)=1.0 and Type I ELMs, with argon seeding (left), and without impurity seeding (reference pulse, right).*

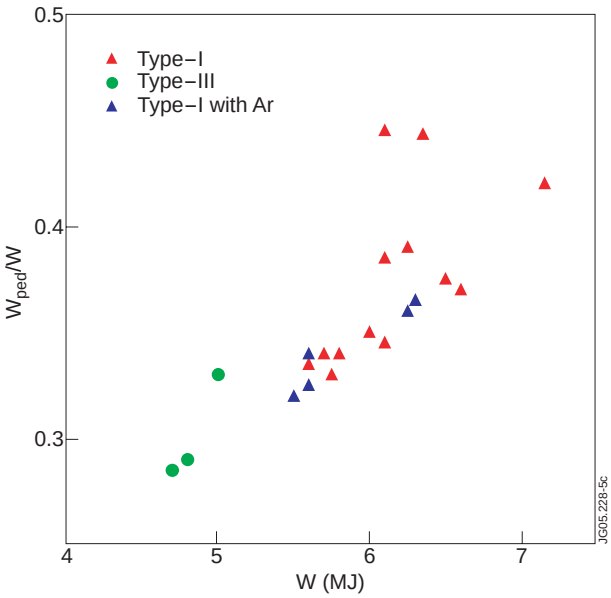


*Figure 4: Fraction of pedestal energy for reference pulses without seeding, and for argon seeded pulses. High triangularity configuration ($\delta \geq 0.4$). The fraction of energy in the pedestal is the same for seeded and non-seeded pulses.*

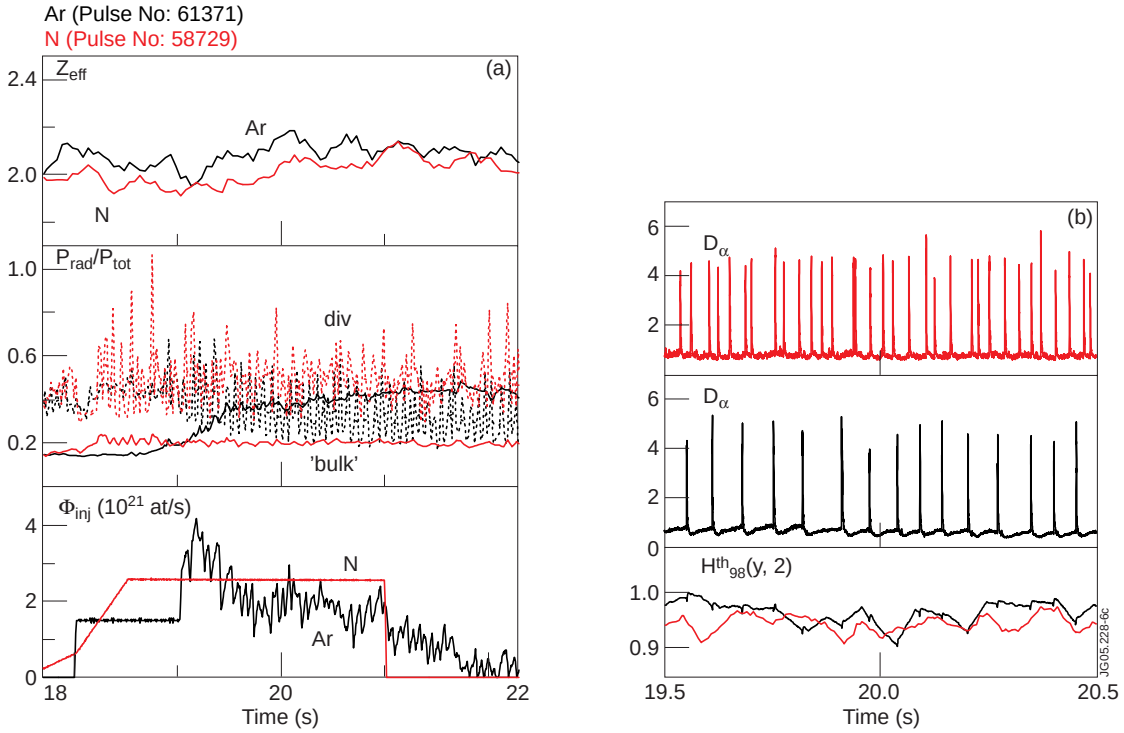


*Figure 6: Comparison of two pulses with Ar seeding (blue trace) and N seeding (green trace), in the same high triangularity configuration, same fractions of Greenwald density, and total radiated power ($P_{rad}/P_{tot}$~0.70). a) line averaged effective charge from visible bremstrahlung measurements, fraction of radiation in the divertor and inside the separatrix, and nitrogen and argon injection rates. b) $D_\alpha$ signature in the divertor, and confinement improvement factor.*

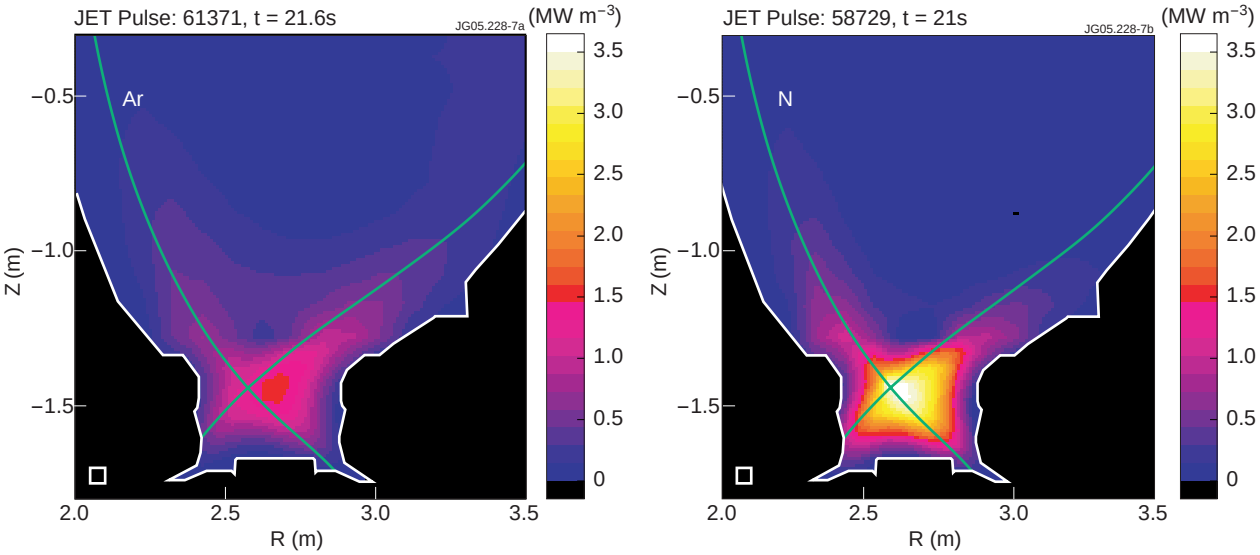


*Figure 7: Bolometric reconstruction of the radiated power density in the X-point region in two pulses shown in Fig.6. (a) with argon seeding, and (b) with nitrogen seeding.*

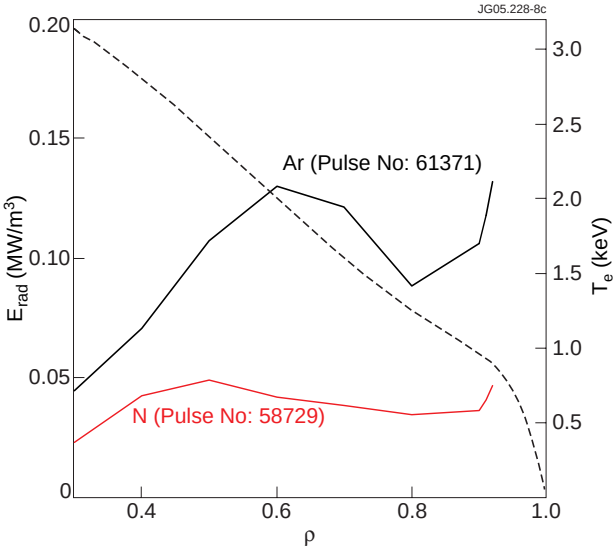


*Figure 8: Radial profiles of the radiated power density for the two pulses shown in Fig.6 and 7. These profiles are obtained from tomographic reconstruction of bolometer data.The electron temperature profile is shown on the left hand side.*

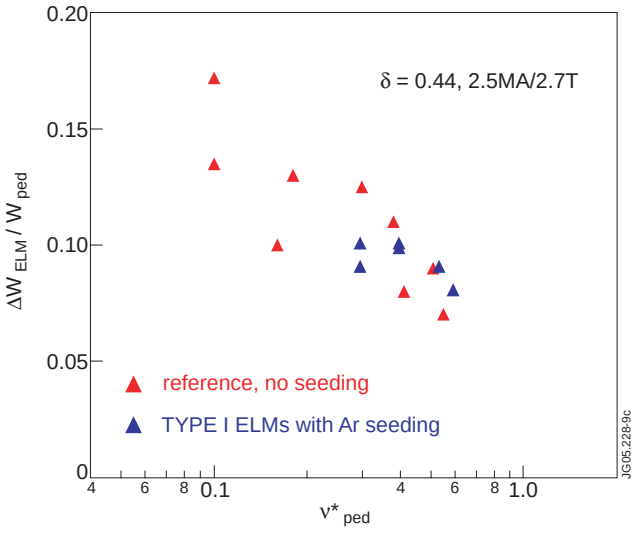


*Figure 9: Normalized plasma energy loss per ELM versus pedestal collisionality for high triangularity H-mode pulses with Type I ELMs. Red triangles: reference pulses without seeding. Blue triangles: Ar seeded H-modes.*

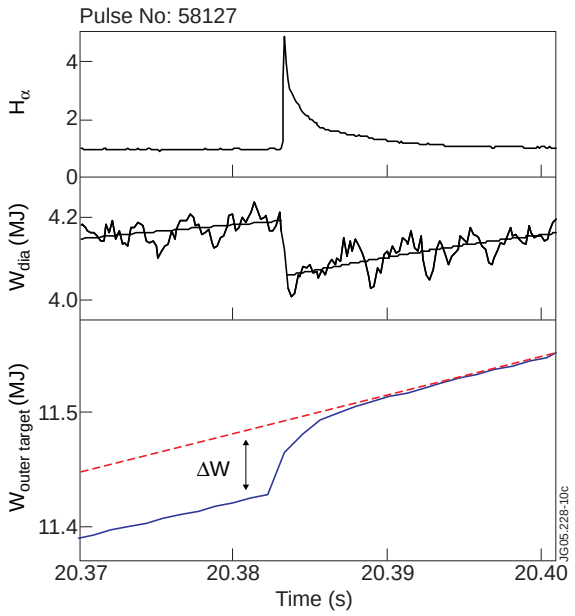


*Figure 10: $D_\alpha$ signal, plasma energy loss and target energy increase during an ELM ($\Delta W_{target}$) deduced from diamagnetic measurements and surface temperature measurements respectively.*

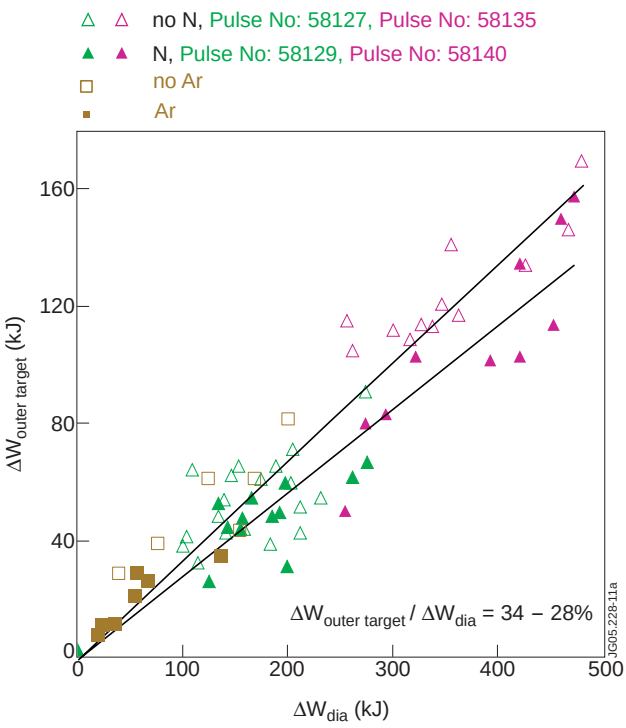


*Figure 11: Energy increase on the outer(left) and inner (right) divertor targets versus plasma energy loss during a Type I ELM. Solid symbols: Ar (squares) or N (triangles) seeding. Open symbols : reference case without seeding.*

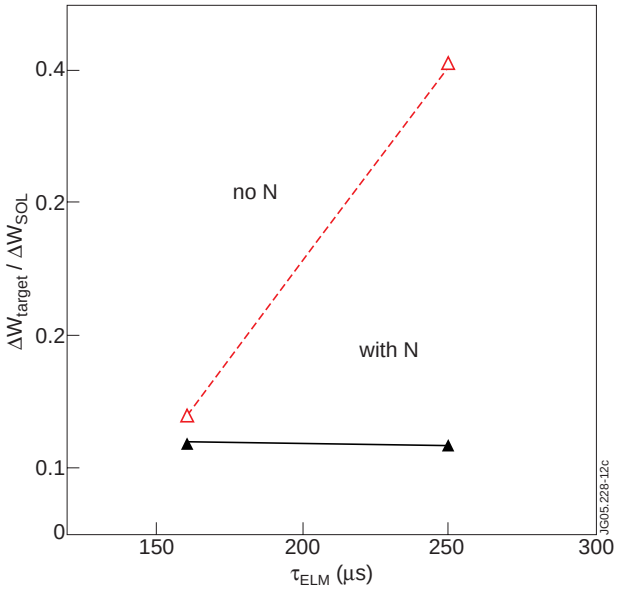


*Figure 12: Integrated electron energy on the target plate normalized to that in the SOL, versus time needed to remove a given energy from the pedestal. Solps5.0 calculation for Pulse No: 58135 (no N) and Pulse No: 58139 (with N).*

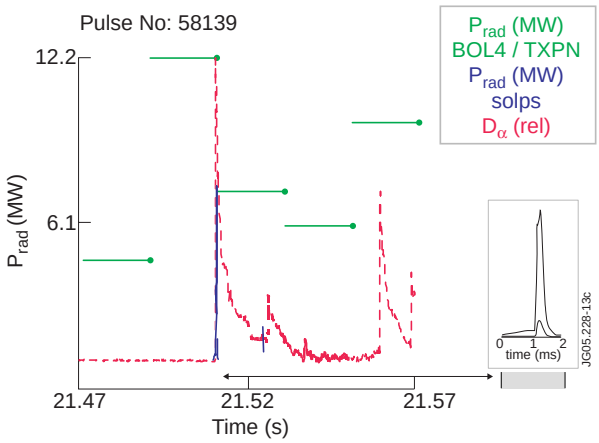


*Figure 13: Time evolution of the measured divertor $H_a$ signal (red), radiation in the X-point and divertor regions from bolometry (green), and N divertor radiation from Solps 5.0 (blue).*